

Parameterized macromodels for lossy multiconductor transmission lines

Original

Parameterized macromodels for lossy multiconductor transmission lines / GRIVET TALOCIA, S., Acquadro, S., Peraldo, C., Canavero, F., Kelander, I., Rouvala, M., Arslan, A.. - STAMPA. - (2006), pp. 93-96. (17th International Zurich Symposium on Electromagnetic Compatibility Singapore Feb. 27 2006-March 3 2006) [10.1109/EMCZUR.2006.214877].

Availability:

This version is available at: 11583/1412874 since: 2015-07-14T10:58:21Z

Publisher:

IEEE

Published

DOI:10.1109/EMCZUR.2006.214877

Terms of use:

This article is made available under terms and conditions as specified in the corresponding bibliographic description in the repository

Publisher copyright

(Article begins on next page)

Parameterized Macromodels for Lossy Multiconductor Transmission Lines

S. Grivet-Talocia¹, S. Acquadro¹, C. Peraldo¹, F. Canavero¹, I. Kelander², M. Rouvala², A. Arslan²

¹Politecnico di Torino, Dip. Elettronica, Torino, Italy. E-mail: grivet@polito.it

²Nokia Research Center, Helsinki, Finland. E-mail: markku.rouvala@nokia.com

Abstract— We present a procedure for the generation of parameterized macromodels for lossy transmission lines. The macromodels are based on delay extraction and rational approximations in the framework of the Generalized Method-of-Characteristics. We extend this existing macromodeling technique to explicitly include the variation of significant geometrical and electrical parameters. Such parameterized macromodels are ideally suited for the automated design of electrical links and for what-if analyses aimed at link optimization, allowing for the inclusion of nonlinear driver and receiver networks and using standard circuit solvers in time domain. We demonstrate the effectiveness of the approach by applying it to flexible printed interconnect structures typically present in cellular phones having moving parts.

I. INTRODUCTION

The design of electronic systems requires several optimization steps to guarantee desired performances. This applies also to electrical interconnects providing the link between drivers and receivers located at different physical locations in the system. These interconnects must insure a correct functional behavior, i.e., safe digital transmission with a negligible bit-error-rate, under all working conditions. The designer is therefore challenged with the choice of the “best” interconnect structure for the particular application. The geometrical and material properties of the interconnect are free variables in this stage, and their number may be quite large, depending on the complexity of the system. It is clear that the performance optimization of the interconnect is greatly simplified and can be automated only when parameterized models representing the electrical behavior and including the effect of parameter variations are available.

The subject of parameterized macromodeling has been addressed in the framework of model order reduction in [1], [2]. In this work, we use a complementary approach by introducing a parameterization scheme for macromodels of lossy multiconductor transmission lines based on the so-called Generalized Method of Characteristics [3], [4]. These models are constructed via extraction of the asymptotic modal delays of the line combined with low-order rational approximations of characteristic admittance and delayless propagation operators. This representation describes the interconnect as a multiport governed by Delayed Ordinary Differential Equation, which can be easily synthesized into an equivalent circuit using only standard elements. Critical interconnect analyses can then be performed in time-domain with real terminations, even transistor-level models of actual drivers and receivers, using a standard circuit solver, like, e.g., SPICE. The accuracy and efficiency of this macromodeling technique

is widely recognized.

The macromodel parameterization scheme is described and developed through an application example. Specifically, we concentrate on a flexible printed interconnect employed in cellular phones having moving parts. The basic structure is depicted in Fig. 1 and described in Section II, where the per-unit-length matrices are reported for several combinations of the geometrical parameters that were considered. Section III describes the proposed parameterization, illustrating its suitability for present application. Numerical results are also presented in Section III.

II. STRUCTURE SPECIFICATION AND CHARACTERIZATION

We consider here the structure depicted in Fig. 1, representing a simplified cross-section of a flexible printed interconnect of a mobile phone. The geometrical parameters (conductor width w and separation d , dielectric thickness h , etc.) and electrical parameters (dielectric constant ϵ_r) are not specified as single values but as ranges of variation, summarized in table I. This is a typical scenario in the early stage of a product development, when the physical design has still to be finalized. All these parameters will be collected in a m -dimensional array $\lambda = (\lambda_1, \dots, \lambda_m)$. In this work, we present preliminary results for a two-dimensional parameter space, with $\lambda_1 = w$ and $\lambda_2 = d/w$, setting $h_2 = 57.5 \mu\text{m}$, $\delta = 0 \text{ mm}$, $\epsilon_r = 3.6$. The line length is assumed $\mathcal{L} = 10 \text{ cm}$. The complete parameterization will be documented in a forthcoming report.

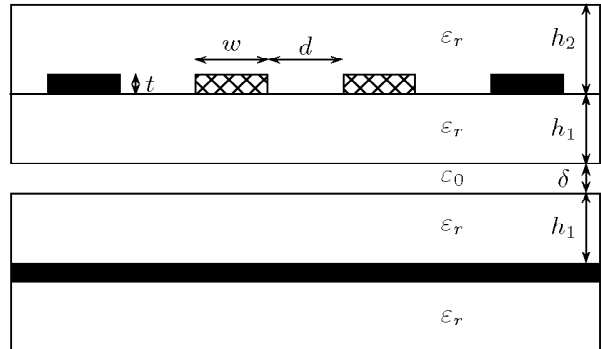


Fig. 1. Cross-section of the transmission-line under investigation. Crosshatch and solid fill indicate signal and ground conductors, respectively. The air-gap δ is generated between two flexible printed circuit layers when the layers are turned and slid over each other in moving mechanisms.

Since the cross-section is translation-invariant, we describe the interconnect as a uniform transmission line governed by parameterized telegraphers' equations

$$\begin{aligned} -\frac{d}{dz}\mathbf{V}(z, s; \lambda) &= [\mathbf{R}(s; \lambda) + s\mathbf{L}(s; \lambda)] \mathbf{I}(z, s; \lambda) \quad (1) \\ -\frac{d}{dz}\mathbf{I}(z, s; \lambda) &= [\mathbf{G}(s; \lambda) + s\mathbf{C}(s; \lambda)] \mathbf{V}(z, s; \lambda) \end{aligned}$$

where s is the Laplace variable and with $\mathbf{G}(s; \lambda)$, $\mathbf{C}(s; \lambda)$, $\mathbf{R}(s; \lambda)$ and $\mathbf{L}(s; \lambda)$ denoting the frequency-dependent parameterized per-unit-length conductance, capacitance, resistance, and inductance matrices, respectively.

The structure was first characterized by computing a frequency sweep of the per-unit-length matrices for some fixed points $\{\lambda^{(1)}, \dots, \lambda^{(p)}\}$ in the parameter space. Five equally-spaced values for both conductor width w and normalized spacing d/w covering the range of interest (see Table I) were considered, leading to a set of $p = 25$ different sets of matrices. In this work we neglect dielectric losses, therefore the conductance matrices are vanishing and the per-unit-length capacitance matrices are constant throughout frequency,

$$\mathbf{G}(s; \lambda) = \mathbf{0}, \quad \mathbf{C}(s; \lambda) = \mathbf{C}(\lambda). \quad (2)$$

The p capacitance matrices were computed by repeated application of the Method-of-Moments (MoM) technique of [5] to the individual geometries. Instead, the full frequency dependence of line resistance and inductance were considered in order to include skin-effect losses. The 2D Green's function of the planar structure was approximated via the procedure outlined in [6]. Then, the discretization of the current density in the conductors using an adaptive and frequency-dependent mesh, combined with a standard 2D MoM formulation, allowed to compute the per-unit-length resistance and inductance matrices over a broad frequency range, from DC up to 10 GHz. Some of the results are reported in Fig. 2. These per-unit-length matrices constitute the raw dataset for the generation of parameterized macromodels of the structure.

III. PARAMETERIZED MACROMODELING

The macromodeling procedure follows from [3], [4], extending all derivations to the parameterized case. The transmission line segment is treated as a multiport, with $\mathbf{V}_1(s; \lambda)$, $\mathbf{I}_1(s; \lambda)$ and $\mathbf{V}_2(s; \lambda)$, $\mathbf{I}_2(s; \lambda)$ denoting the near and far end terminal voltage and current vectors. The dependence of network quantities on s and λ will be omitted in the following. In the framework of the

TABLE I
PARAMETERS RANGE OF VARIATION.

Parameter	Min	Max
h_1	50 μm	50 μm
h_2	50 μm	65 μm
δ	0 mm	1 mm
w	50 μm	150 μm
d	w	$2w$
t	17.5 μm	17.5 μm
ε_r	3.2	4.0
Length	0 mm	300 mm

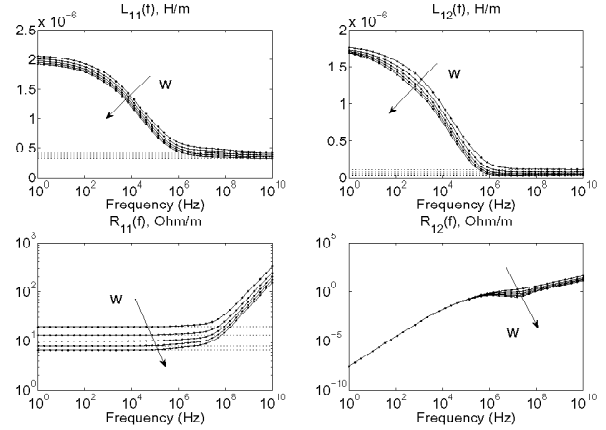


Fig. 2. Per-unit-length resistance and inductance plotted versus frequency. The arrows indicate increasing values of w from 50 μm to 150 μm . In all plots $d/w = 1.5$. Horizontal dotted lines denote asymptotic values (DC resistances and high-frequency inductances).

Generalized Method of Characteristics, the solution of Eqs. (1) can be restated as

$$\mathbf{I}_1 = \mathbf{Y}_c(s; \lambda)\mathbf{V}_1 - \mathbf{J}_1 \quad (3)$$

$$\mathbf{I}_2 = \mathbf{Y}_c(s; \lambda)\mathbf{V}_2 - \mathbf{J}_2$$

where

$$\mathbf{J}_1 = \mathbf{H}(s; \lambda) [\mathbf{Y}_c(s; \lambda)\mathbf{V}_2 + \mathbf{I}_2] \quad (4)$$

$$\mathbf{J}_2 = \mathbf{H}(s; \lambda) [\mathbf{Y}_c(s; \lambda)\mathbf{V}_1 + \mathbf{I}_1]$$

and with

$$\begin{aligned} \Gamma^2(s; \lambda) &= [\mathbf{G}(s; \lambda) + s\mathbf{C}(s; \lambda)] [\mathbf{R}(s; \lambda) + s\mathbf{L}(s; \lambda)] \\ \mathbf{Y}_c(s; \lambda) &= \Gamma^{-1}(s; \lambda) [\mathbf{G}(s; \lambda) + s\mathbf{C}(s; \lambda)] \\ \mathbf{H}(s; \lambda) &= e^{-\mathcal{L}\Gamma(s; \lambda)} \end{aligned} \quad (5)$$

being the squared propagation matrix, the characteristic admittance matrix, and the propagation operator for a line length \mathcal{L} , respectively.

The key point enabling the construction of a macromodel suitable for time-domain analysis is the approximation of $\mathbf{Y}_c(s; \lambda)$ and $\mathbf{H}(s; \lambda)$ as a combination of rational functions of frequency and pure delay terms. In fact, this approximation leads naturally to a system of Delayed Ordinary Differential Equations, and allows the macromodel to be synthesized into an equivalent circuit using only standard elements (if not directly available, pure delays can be synthesized by matched ideal lossless transmission lines). A complete description is found in [4]. The main difficulty we deal with in this work is the parameterization of such delayed rational approximations. This step is described next.

The set of parameter-dependent modal delays are computed as $T_k(\lambda) = \mathcal{L} \sqrt{\Lambda_k(\lambda)}$, given the asymptotic eigendecomposition

$$\text{diag}\{\Lambda_k(\lambda)\} = \mathbf{M}_\infty^{-1} \mathbf{C}(\infty; \lambda) \mathbf{L}(\infty; \lambda) \mathbf{M}_\infty. \quad (6)$$

Matrix \mathbf{M}_∞ provides the high-frequency propagation modes of the structure. Note that for the structure of Fig. 1, these modes (actually even and odd modes) are not dependent on frequency and also not dependent on any

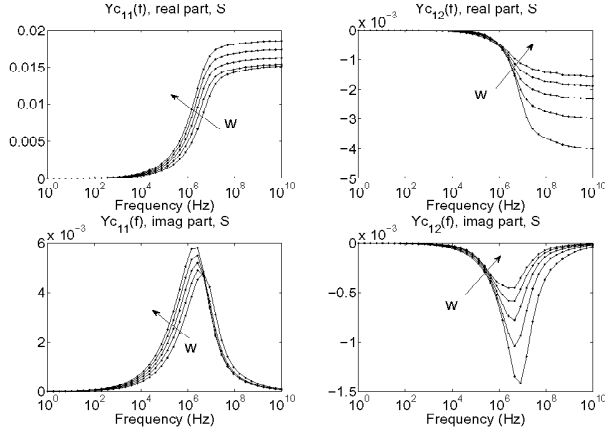


Fig. 3. Selected entries of $\mathbf{Y}_c(s; \lambda)$ plotted versus frequency for various parameter configurations. The arrows indicate increasing values of w from $50 \mu\text{m}$ to $150 \mu\text{m}$. In all plots $d/w = 1.5$.

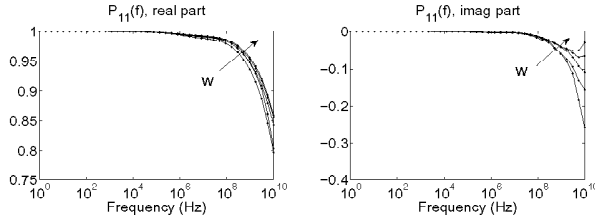


Fig. 4. Selected entries of $\mathbf{P}(s; \lambda)$ plotted versus frequency for various parameter configurations. The arrows indicate increasing values of w from $50 \mu\text{m}$ to $150 \mu\text{m}$. In all plots $d/w = 1.5$.

of the parameters in λ , since the symmetry of the cross-section is preserved uniformly in the parameter space. This allows the definition of a delayless propagation operator

$$\mathbf{P}(s; \lambda) = \text{diag}\{e^{sT_k(\lambda)}\} \mathbf{M}_\infty^{-1} \mathbf{H}(s; \lambda) \mathbf{M}_\infty. \quad (7)$$

which results diagonal at all frequencies. The asymptotic modal delays are compensated in (7) by the pre-multiplication by the diagonal matrix $\text{diag}\{e^{sT_k(\lambda)}\}$, so that the operator $\mathbf{P}(s; \lambda)$ mainly represents only line dispersion and attenuation.

Once the delay terms have been extracted, rational approximations of $\mathbf{Y}_c(s; \lambda)$ and $\mathbf{P}(s; \lambda)$ are computed. During this phase, also a suitable interpolation scheme must be devised for the representation of such approximations over the entire parameter space, given the finite number p of samples that is actually available. Figures 3-4 show the frequency dependence of some entries of the matrices to be approximated/interpolated. From these plots we see that the frequency dependence is very smooth, thus confirming the feasibility of a rational approximation. Note that also the variations induced by the parameters are very smooth.

We chose the following representation

$$\begin{aligned} \mathbf{Y}_c(s; \lambda) &\simeq \sum_n \frac{\mathbf{R}_n^Y(\lambda)}{s - p_n} + \mathbf{Y}_\infty(\lambda) \\ \mathbf{P}(s; \lambda) &\simeq \sum_n \frac{\mathbf{R}_n^P(\lambda)}{s - q_n} + \mathbf{P}_\infty(\lambda), \end{aligned} \quad (8)$$

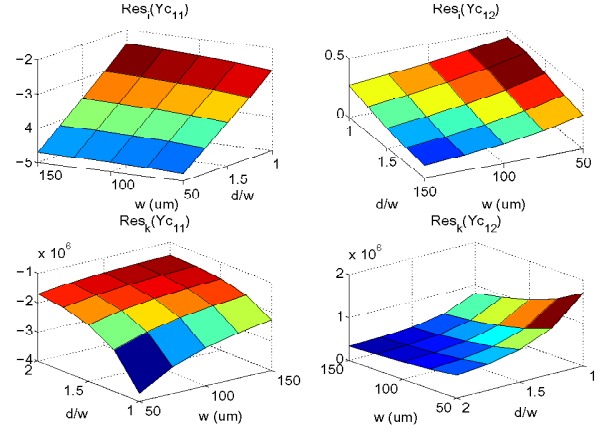


Fig. 5. Parameter-induced variations on two of the residue matrices in the rational approximation of the characteristic admittance $\mathbf{Y}_c(s; \lambda)$. Top row: low-frequency pole; Bottom row: high-frequency pole.

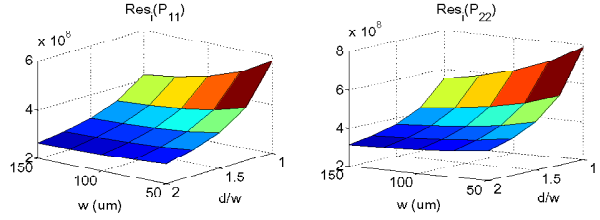


Fig. 6. Parameter-induced variations on one of the residue matrices in the rational approximation of the propagation operator $\mathbf{P}(s; \lambda)$.

characterized by common poles. The computation of these poles was performed by applying the well-known Vector Fitting algorithm [7]. In order to maximize accuracy, the entire set of p realizations was included in a single run. This was possible due to the limited number of available frequency samples (40). However, almost identical poles were obtained using a restricted set of realizations using all combinations of upper and lower bound for each parameter. This low sensitivity justifies the use of common poles in (8).

Residues and direct coupling matrices in (8) were computed via separate linear least squares problems for each of the p parameter combinations. A continuous variation throughout the parameter space can be recovered as

$$\mathbf{R}_n^Y(\lambda) = \sum_\nu \theta_n^\nu \mathbf{R}_n^Y(\lambda^{(\nu)}), \quad (9)$$

and similarly for the other parameter-dependent matrices in (8), where the coefficients θ_n^ν are determined by multi-dimensional linear (bilinear for present application) interpolation, using only the two nearest neighbors bracketing the desired value of λ along each of its scalar components.

Figures 5 and 6 represent the typical variation of the residue matrices with respect to the parameters λ . These figures confirm the smoothness of the residues with respect to λ , therefore justifying the use of a linear interpolation. Even if higher-order approximations are possible, we believe that the accuracy level of a linear scheme is sufficient for present application. Figure 7 represents the even/odd modal delays $T_k(\lambda)$ that were

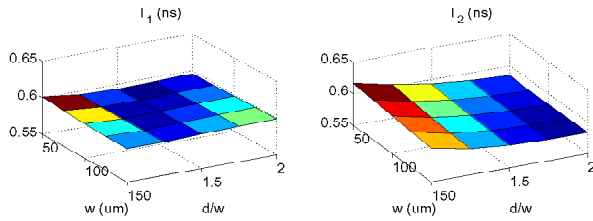


Fig. 7. Parameter-induced variations on modal delays (T_1 : even mode, T_2 : odd mode).

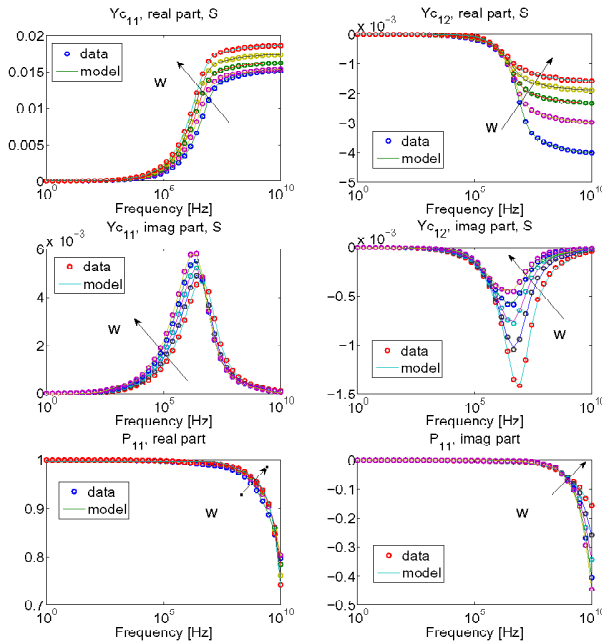


Fig. 8. Parametric rational approximation of characteristic admittance and propagation operator. Parameter values as in Fig. 3.

computed, explicitly showing their parametric dependence. As expected, the delay variation is very limited. Nonetheless, we apply the same linear interpolation scheme to represent the continuous variation of the delays.

As a validation, we report in Fig. 8 a comparison of raw frequency-dependent data and parametric model fit for some parameter configuration. A total number of 8 and 5 poles were used for the characteristic admittance and propagation operator, respectively. These plots illustrate the uniform accuracy that is achieved by the rational approximations (8), even using a limited number of common poles. Similar results were obtained for all other matrix entries and for any combination of the parameters.

A final remark on the implementation of the parameterized macromodels into a standard circuit solver. The circuit synthesis of the macromodel based on (3)-(8) has already been solved and discussed in [3], [4] for a fixed value of the parameters λ . Such macromodel is easily cast as a library block or subcircuit to be called by the solver (e.g., .SUBCKT if using SPICE). The only difference induced by the parameterization is the dependence of the various circuit elements on each of the parameters in λ . Due to the adopted linear interpolation scheme, the variation law can be easily hard-coded in the

definition of the circuit elements. Therefore, the actual circuit implementation step poses no particular difficulty.

IV. CONCLUSION

We have presented a procedure for including the effects of varying electrical and geometrical parameters in macromodels of lossy transmission-lines. A combination of delay extraction and rational approximations of suitable transfer functions of the lines allows to cast the macromodels in a form that is accepted by any standard circuit solver, like, e.g., SPICE. On the other hand, the specific model representation, which is based on an extension of the well-known Method-of-Characteristics, leads to a very smooth dependence on the relevant geometrical and electrical parameters of the structure. In particular, we have shown that a common set of poles is able to approximate very accurately both characteristic admittance and propagation operators over the entire parameter space. Consequently, simple linear interpolation schemes can be applied only to residue and delay matrices in order to represent the electrical behavior of the structure over the entire parameter space.

The proposed modeling scheme is here applied to the representation of flexible printed interconnects present in modern cellular phones having moving parts. The resulting accuracy is excellent throughout the parameter space for all interconnects that were analyzed. The availability of accurate parameterized macromodels for such interconnects will allow systematic analysis of critical electrical links in time-domain with realistic (nonlinear/dynamic) driver and receiver networks. This in turn will allow link optimization under signal integrity constraints, with a consequent speedup in the overall interconnect design process.

REFERENCES

- [1] P. Gunupudi, R. Khazaka, M. Nakhla, "Analysis of transmission line circuits using multidimensional model reduction techniques" *IEEE Trans. Adv. Packaging*, Vol. 25, N. 2, May 2002, pp. 174-180.
- [2] P. K. Gunupudi, R. Khazaka, M. S. Nakhla, T. Smy, D. Celso, "Passive parameterized time-domain macromodels for high-speed transmission-line networks" *IEEE Trans. Microwave Theory and Techniques*, Vol. 51, N. 12, Dec. 2003, pp. 2347-2354.
- [3] S. Grivet-Talocia, F. G. Canavero, "TOPLINE: a delay-pole-residue method for the simulation of lossy and dispersive interconnects", in *Digest of Electr. Perf. Electronic Packaging*, Vol. 11, Monterey, CA, October 2002, pp. 359-362.
- [4] S. Grivet-Talocia, H. M. Huang, A. E. Ruehli, F. Canavero, I. M. Elfadel, "Transient Analysis of Lossy Transmission Lines: an Effective Approach Based on the Method of Characteristics", *IEEE Trans. Advanced Packaging*, pp. 45-56, vol. 27, n. 1, Feb. 2004.
- [5] C. Wei, R. F. Harrington, J. R. Mautz, T. Sarkar, "Multiconductor Transmission Lines in Multilayered Dielectric Media", *IEEE Trans. Microwave Theory and Techniques*, Vol. 32, N. 4, Apr. 1984, pp. 439-450.
- [6] K. M. Coperich, J. Morsey, V. I. Okhmatovski, A. C. Cangellaris, A. E. Ruehli, "Systematic development of transmission-line models for interconnects with frequency-dependent losses" *IEEE Trans. Microwave Theory and Techniques*, Vol. 49, N. 10, Oct. 2001, pp. 1677-1685.
- [7] B. Gustavsen, A. Semlyen, "Rational approximation of frequency domain responses by vector fitting", *IEEE Trans. Power Delivery*, Vol. 14, 1999, pp. 1052-1061.